

Raman scattering study of delafossite magnetoelectric multiferroic compounds: CuFeO_2 and CuCrO_2

This article has been downloaded from IOPscience. Please scroll down to see the full text article.

2012 J. Phys.: Condens. Matter 24 036003

(<http://iopscience.iop.org/0953-8984/24/3/036003>)

View [the table of contents for this issue](#), or go to the [journal homepage](#) for more

Download details:

IP Address: 137.205.50.42

The article was downloaded on 02/06/2012 at 14:50

Please note that [terms and conditions apply](#).

Raman scattering study of delafossite magnetoelectric multiferroic compounds: CuFeO_2 and CuCrO_2

O Aktas¹, K D Truong², T Otani³, G Balakrishnan⁴, M J Clouter¹,
T Kimura³ and G Quirion¹

¹ Department of Physics and Physical Oceanography, Memorial University, St Johns, NF, A1B 3X7, Canada

² Département de Physique, Université de Sherbrooke, Sherbrooke, Canada

³ Division of Material Physics, Graduate School of Engineering Science, Osaka University, Toyonaka, Japan

⁴ Department of Physics, University of Warwick, Coventry, UK

E-mail: oktay@mun.ca

Received 7 October 2011, in final form 18 November 2011

Published 9 December 2011

Online at stacks.iop.org/JPhysCM/24/036003

Abstract

Ultrasonic velocity measurements on the magnetoelectric multiferroic compound CuFeO_2 reveal that the antiferromagnetic transition observed at $T_{\text{N}1} = 14$ K might be induced by an $R\bar{3}m \rightarrow C2/m$ pseudoproper ferroelastic transition [1]. In that case, the group theory states that the order parameter associated with the structural transition must belong to a two-dimensional irreducible representation $E_g (x^2 - y^2, xy)$. Since this type of transition can be driven by a Raman E_g mode, we performed Raman scattering measurements on CuFeO_2 between 5 and 290 K. Considering that the isostructural multiferroic compound CuCrO_2 might show similar structural deformations at the antiferromagnetic transition $T_{\text{N}1} = 24.3$ K, Raman measurements have also been performed for comparison. At ambient temperature, the Raman modes in CuFeO_2 are observed at $\omega_{E_g} = 352 \text{ cm}^{-1}$ and $\omega_{A_{1g}} = 692 \text{ cm}^{-1}$, while these modes are detected at $\omega_{E_g} = 457 \text{ cm}^{-1}$ and $\omega_{A_{1g}} = 709 \text{ cm}^{-1}$ in CuCrO_2 . The analysis of the temperature dependence of the modes in both compounds shows that the frequencies of all modes increase with decreasing temperature. This typical behavior is attributed to anharmonic phonon–phonon interactions. These results clearly indicate that none of the Raman active modes observed in CuFeO_2 and CuCrO_2 drive the pseudoproper ferroelastic transitions observed at the Néel temperature $T_{\text{N}1}$. Finally, a broad band at about 550 cm^{-1} observed in the magnetoelectric phase of CuCrO_2 below $T_{\text{N}2}$ could be associated with magnons.

(Some figures may appear in colour only in the online journal)

1. Introduction

CuFeO_2 and CuCrO_2 belong to the delafossite frustrated antiferromagnets with the chemical formula ABO_2 in which A is a nonmagnetic monovalent ion (Cu or Ag) while B is a magnetic trivalent ion such as Fe or Cr [2–5]. Some of these compounds, including AgCrO_2 , CuFeO_2 , and CuCrO_2 , belong to the trigonal $R\bar{3}m$ space group at room temperature and undergo a series of magnetic phase transitions [3–5] at

low temperatures as a result of geometrical frustration of magnetic ions on a triangular lattice.

In the case of CuFeO_2 , two antiferromagnetic transitions are observed at zero field. In its ground state Fe^{3+} ions order into a collinear commensurate four-sublattice ($\uparrow\uparrow\downarrow\downarrow$) structure, while between $T_{\text{N}2} = 11$ K and $T_{\text{N}1} = 14$ K the magnetic order is incommensurate, with the magnetic moments also pointing along the c -axis [6]. With the application of a field parallel to the c -axis, a series of new

magnetic orders is stabilized below T_{N2} . At magnetic fields between 7 Tesla (T) and 13 T, CuFeO₂ shows a proper screw spin configuration where the spins lie in the $R\bar{3}m$ mirror plane perpendicular to the magnetic modulation vector $\mathbf{q} \parallel [110]$ (hexagonal basis) [2, 4, 7, 8]. At higher fields, several other spin configurations are observed: a c -axis collinear five-sublattice ($\uparrow\uparrow\downarrow\downarrow$) state ($13 \text{ T} < H < 20 \text{ T}$), a c -axis collinear three-sublattice ($\uparrow\uparrow\downarrow$) structure ($20 \text{ T} < H < 34 \text{ T}$), a canted three-sublattice state ($34 \text{ T} < H < 49 \text{ T}$), and a noncollinear incommensurate spin-flop phase, which is close to the 120° spin structure for $49 \text{ T} < H < 70 \text{ T}$, followed by a transition to the paramagnetic state at 70 T [4, 9].

While CuCrO₂ is isostructural to CuFeO₂ at room temperature, its magnetic phase diagram is significantly different [3, 5, 10]. According to specific heat and magnetic susceptibility measurements [5], CuCrO₂ shows anomalies at $T_{N1} = 24.3 \text{ K}$ and $T_{N2} = 23.6 \text{ K}$. The magnetic order in the intermediate temperature range $T_{N1} < T < T_{N2}$ is interpreted as a collinear state with $\mathbf{S} \parallel c$ [5], while recent neutron diffraction measurements [11, 12] reveal an incommensurate proper screw spin structure with $\mathbf{q} \parallel [110]$ below T_{N2} . This spin configuration is very similar to the one observed in CuFeO₂ at applied fields between 7 and 13 T. Moreover, additional studies on both compounds [2, 3, 5] show that an electric polarization $\mathbf{P} \parallel [110]$ is only induced upon the emergence of this proper screw spin order. Under this scenario, the usual inverse Dzyaloshinskii–Moriya (DM) interaction $\mathbf{P} \sim \mathbf{r}_{ij} \times (\mathbf{S}_i \times \mathbf{S}_j)$ [13, 14] cannot account for the induced polarization because the q -vector of the spin modulation is perpendicular to the spiral plane. An alternative possibility, proposed by Arima *et al* [15], is that the polarization is induced by spin–orbit coupling. Thus, CuFeO₂ and CuCrO₂ represent a different class of magnetoelectric multiferroics in which the mechanism leading to the magnetoelectric coupling is still uncertain.

Other particular properties of CuFeO₂ have also been recently revealed via sound velocity measurements [1, 4, 16]. These measurements show softening on specific elastic constants as the temperature is decreased to $T_{N1} = 14 \text{ K}$. The data analysis indicates that this peculiar behavior is characteristic of an $R\bar{3}m \rightarrow C2/m$ pseudoproper ferroelastic transition, consistent with neutron [17] and x-ray [7] diffraction measurements. Furthermore, according to group theory [18], the order parameter associated with the structural transition must belong to a two-dimensional irreducible representation (IR) $E_g(x^2 - y^2, xy)$. Given that none of the spin components belong to this IR, these measurements indicate that the magnetic order in CuFeO₂ is stabilized by the ferroelastic structural transition, thereby suggesting a possible role played by the spin–lattice coupling in this family of multiferroic materials. Thus, the true origin of the structural transition observed at T_{N1} remains a mystery. One possibility is that the transition is driven by a Raman mode as in other pseudoproper ferroelastic materials [19–22]. Regarding isostructural CuCrO₂, recent magnetostriction measurements [23] show evidence for a structural phase transition at $T_{N1} = 24.3 \text{ K}$. Furthermore, as preliminary sound velocity measurements on CuCrO₂ (shown in figure 1)

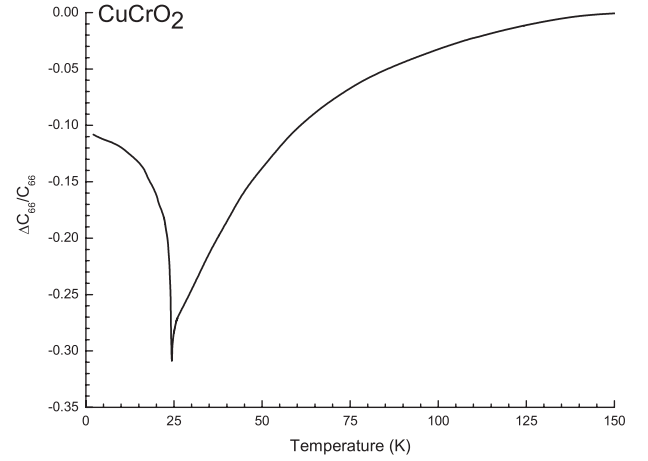


Figure 1. Relative variation of the elastic constant C_{66} in CuCrO₂ as a function of temperature obtained by sound velocity measurements. C_{66} shows a 30% reduction at $T_{N1} = 24.3 \text{ K}$ relative to the value at 150 K, indicating that the antiferromagnetic transition at T_{N1} might also be ferroelastic.

reveal softening similar to that observed in CuFeO₂ [1], the transition observed at $T_{N1} = 24.3 \text{ K}$ in CuCrO₂ might also be ferroelastic. In order to possibly identify the order parameter associated with these pseudoproper ferroelastic transitions, we performed Raman scattering measurements on the isostructural compounds CuFeO₂ and CuCrO₂. The remainder of the paper is organized as follows. Experimental methods are discussed in section 2 while results and discussion are presented in section 3. Finally, conclusions are made in section 4.

2. Experiment

Single crystals of CuFeO₂ were grown by the floating zone method using a four mirror image furnace [24]. CuFeO₂ samples used in the measurements had an area of $\sim 2 \text{ mm} \times \sim 2 \text{ mm}$ and was $\sim 1 \text{ mm}$ in length along the c -axis. Single crystals of CuCrO₂ were grown from Bi₂O₃ flux [5]. The samples were platelets with a length of 0.4 mm along the c -axis. The surface area was approximately $2 \text{ mm} \times 2 \text{ mm}$. Prior to Raman scattering experiments, samples were polished using an abrasive slurry with 50 nm Al₂O₃ grains in order to minimize surface scattering. Room temperature Raman measurements were performed using two different experimental setups. When using an Ar⁺ laser operating at 514.5 nm, the Raman spectra were collected by a double grating spectrometer (Spex Industries, model 1401), a photomultiplier tube (Perkin Elmer, MP 900 series), and a photon counter (Princeton Applied Research, model 1109). For CuCrO₂, 28 mW of exciting beam power was used while it was increased to 50 mW to obtain the spectra of CuFeO₂. For cross-polarization measurements on CuFeO₂, the beam power was increased to 100 mW, which caused local heating on the sample. In the second setup, the 0.5 cm^{-1} resolution micro-Raman measurements were performed with a 632 nm He–Ne laser, a double grating spectrometer (Jobin Yvon, model Labram-800) and a liquid-nitrogen cooled CCD

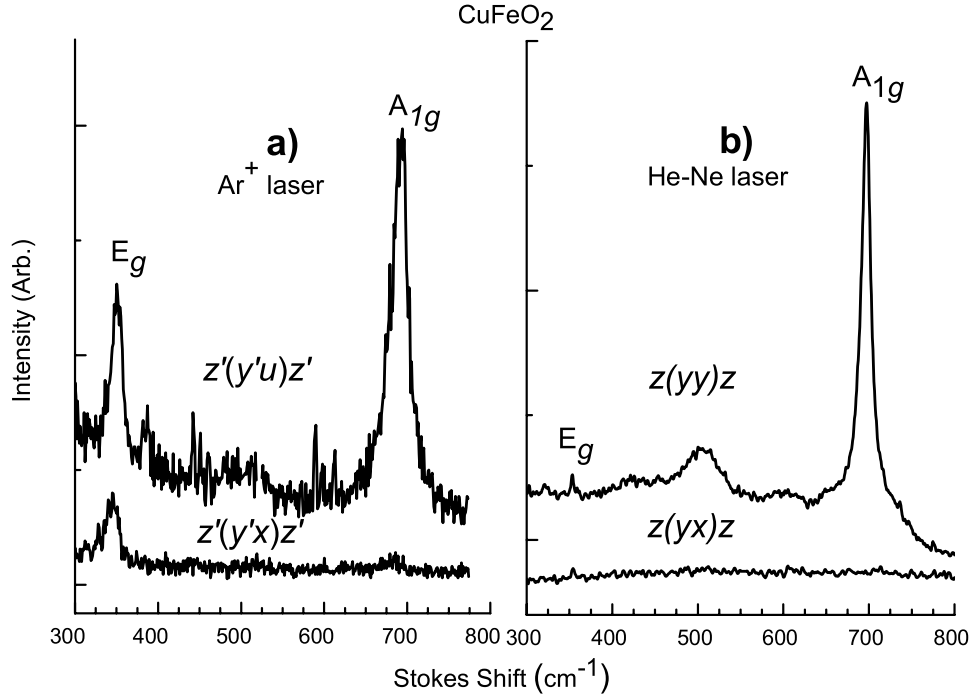


Figure 2. Polarized Raman spectra of CuFeO₂ at room temperature obtained using the Ar⁺ and He-Ne lasers. Experimental scattering geometries are represented by the Porto notation above each spectrum. Polarizations along the y' and x axes are parallel and perpendicular to the plane of incidence, respectively. A strong plasma emission line at 521 cm⁻¹ in the z'(y'u)z' spectrum was removed for clarity. Raman modes with A_{1g} and E_g symmetries are located at ω_{A_{1g}} = 692 cm⁻¹ and ω_{E_g} = 351 cm⁻¹, respectively.

detector. In order to minimize sample heating, 0.3 mW incident beam power with a 3 μm spot size (4000 W cm⁻²) was used. Mode parameters were obtained by a fit to the data using Lorentzian functions for the observed modes.

3. Experimental results and discussion

3.1. Raman spectra of CuFeO₂ and CuCrO₂ at room temperature

Delafossite compounds (space group $R\bar{3}m$) such as CuFeO₂ and CuCrO₂ have one formula unit per unit cell with a total of 12 possible vibrational modes. Among these modes only two are Raman active with E_g and A_{1g} symmetry. The A_{1g} mode corresponds to vibrations of the Cu-O bonds along the c-axis while the E_g mode represents vibrations in the triangular lattice perpendicular to the c-axis. The atomic displacements for these modes are illustrated in [25]. In order to determine the symmetry of the modes observed in CuFeO₂ (figure 2) and CuCrO₂ (figure 3), we performed polarized Raman scattering measurements at room temperature using two different laser sources. Here, Raman scattering geometries are identified using the Porto notation $k_i(e_i e_s)k_s$. The labels z' and y' designate directions making an angle θ relative to the z and y axes, where θ = 50° for CuFeO₂ while θ = 15° for CuCrO₂.

To our knowledge, no polarized Raman measurements on CuFeO₂ single crystals have been reported. At room temperature, the spectrum taken with the Ar⁺ laser using unpolarized (u) scattered light, figure 2(a), shows modes at 349 and 690 cm⁻¹ in agreement with results obtained on polycrystals [26, 27]. The intensity of the mode at 690 cm⁻¹

disappears with cross- (y'x) polarization while the mode at 349 cm⁻¹ remains visible in both (y'u) and cross- (y'x) polarizations. Measurements with the He-Ne laser show Raman modes at 351 and 692 cm⁻¹ and a broad band at 496 cm⁻¹ (see figure 2(b)). The mode at 692 cm⁻¹ has a strong intensity in the parallel polarization (yy) and disappears in the cross-polarization (yx). The intensity of the mode at 351 cm⁻¹ is very weak, which implies that the He-Ne excitation line at 632.8 nm is not in resonance with the vibrations associated with this mode as observed in LiNiO₂ [28]. Despite its weak intensity, it is visible in both polarizations. Moreover, this mode was reproducible down to low temperatures (see figure 4(b)). According to the Raman scattering tensors associated with the trigonal point group $\bar{3}m$ [29],

$$A_{1g}(x) = \begin{bmatrix} a & 0 & 0 \\ 0 & a & 0 \\ 0 & 0 & b \end{bmatrix} \quad (1)$$

and

$$E_g(x) = \begin{bmatrix} c & 0 & 0 \\ 0 & -c & d \\ 0 & d & 0 \end{bmatrix}, \quad E_g(y) = \begin{bmatrix} 0 & -c & -d \\ -c & 0 & 0 \\ -d & 0 & 0 \end{bmatrix}, \quad (2)$$

a cross polarization configuration such as z(yx)z allows only E_g modes, while a parallel polarization configuration such as z(xx)z allows the observation of E_g and A_{1g} modes. Therefore, the mode symmetry is assigned as ω_{A_{1g}} = 692 cm⁻¹ and ω_{E_g} = 351 cm⁻¹.

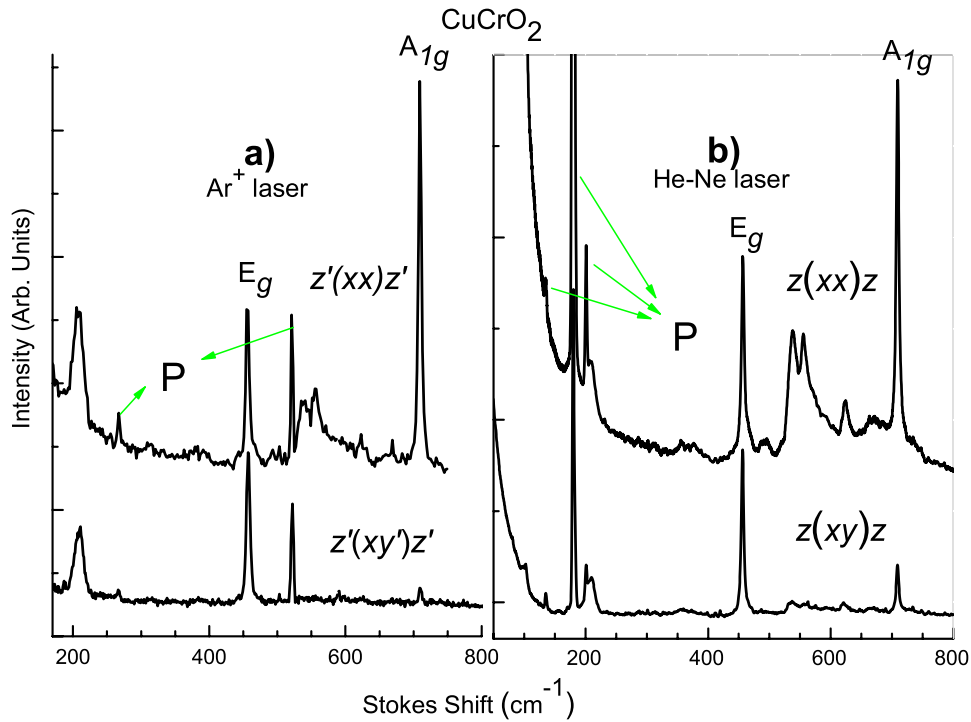


Figure 3. Polarized Raman spectra of CuCrO₂ at room temperature obtained using the Ar⁺ and He-Ne lasers. Experimental scattering geometries are designated by the Porto notation above each spectrum. Polarizations along the *y'* and *x* axes are parallel and perpendicular to the plane of incidence, respectively. Green arrows indicate plasma emission lines (P). Raman modes have frequencies at $\omega_{E_g} = 457 \text{ cm}^{-1}$ and $\omega_{A_{1g}} = 709 \text{ cm}^{-1}$.

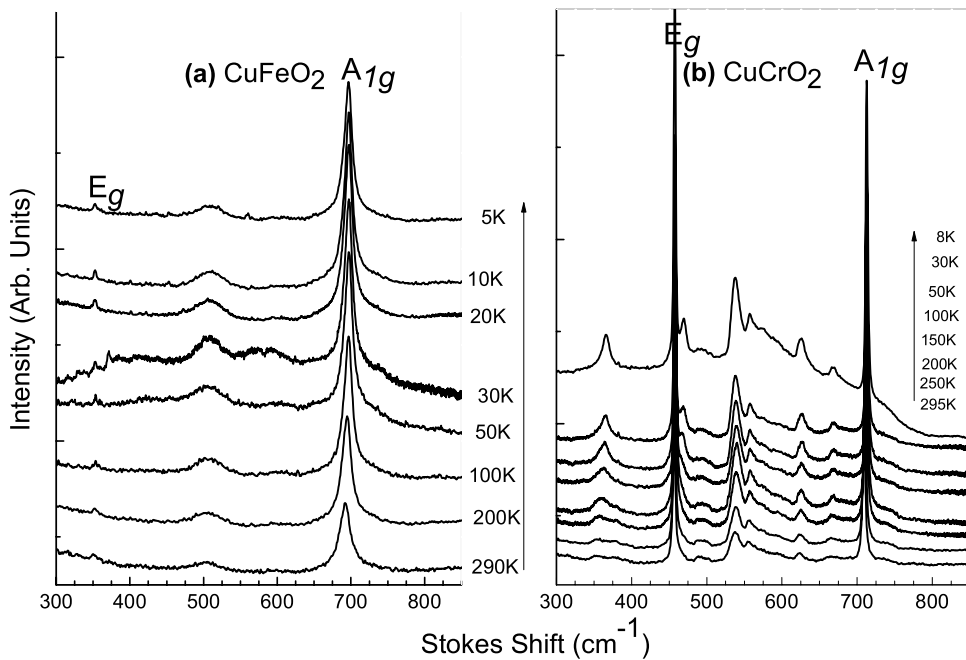


Figure 4. Raman spectra of (a) CuFeO₂ and (b) CuCrO₂ between 5 and 290 K. While no significant change is observed in the CuFeO₂ spectra in this temperature range, an additional mode in CuCrO₂ appears at 467 cm⁻¹ below 200 K and slightly increases in frequency at lower temperatures. In addition, the Raman spectrum of CuCrO₂ at 8 K shows a broad band centered at 550 cm⁻¹. This mode could be due to magnon modes reflecting the proper screw spin structure below $T_{N2} = 23.6 \text{ K}$ in CuCrO₂.

In addition to the vibrational modes observed in CuFeO₂, a broad band located at 496 cm⁻¹ is also revealed using both laser sources. In the unpolarized (*y'u*) spectrum obtained

with the Ar⁺ laser, the intensity of this feature is within the background noise. In the parallel polarized spectrum obtained with the He-Ne laser, the broad peak is clearly observed and

detected down to 5 K (figure 4). Polarized spectra obtained with both excitation lines show that the mode at 496 cm^{-1} has an A_{1g} symmetry. The possible origin of this band will be discussed later.

As in the case of CuFeO_2 , CuCrO_2 should show two Raman modes. However, with unpolarized (u) scattered light (not shown) or a parallel polarization (xx) configuration with the Ar^+ laser (figure 3(a)), we observe modes at 104, 207, 382, 457, 538, 557, 623, 668, and 709 cm^{-1} . When using the He–Ne laser (figure 3(b)), a similar spectrum is obtained except that the mode at 382 cm^{-1} is absent and an additional mode appears at 359 cm^{-1} . The symmetries of these modes can be assigned according to the polarized Raman measurements shown in figure 3. Since the modes at 104, 212, and 457 cm^{-1} are observed in both parallel and cross-polarized Raman spectra, these modes belong to the E_g irreducible representation (IR). The other modes are therefore assigned to A_{1g} IR since their intensities either are weak or disappear in the cross-polarization configuration. So far, there have been four publications reporting Raman spectra of CuCrO_2 powder samples [30–33]. Two of these publications show modes at 207, 444, and 691 cm^{-1} [30, 31]. In addition, one of these works shows additional features with weak intensities at 540 and 560 cm^{-1} [31]. Other publications [32, 33] reveal Raman modes only at 452 and 703 cm^{-1} . By comparison, our polarized Raman results indicate that the Raman modes in CuCrO_2 correspond to $\omega_{A_{1g}} = 709\text{ cm}^{-1}$ and $\omega_{E_g} = 457\text{ cm}^{-1}$.

As mentioned earlier, CuFeO_2 and CuCrO_2 should only have two Raman modes. However, both compounds show additional features (figures 2 and 3) similar to those observed in other delafossite compounds such as CuAlO_2 [34] and CuGaO_2 [25]. In agreement with *ab initio* calculations, these additional modes in CuAlO_2 are attributed to non-zero wavevector phonons which are normally forbidden by Raman selection rules [34]. As suggested, the selection rules are possibly relaxed by defects such as Cu vacancies, interstitial oxygens or tetrahedrally coordinated Cr^{3+} or Fe^{3+} on the Cu site [34]. Thus, the additional features observed in CuFeO_2 and CuCrO_2 could have an origin similar to that observed in CuAlO_2 [34] and CuGaO_2 [25]. They could also be related to crystal field excitations which were revealed in Raman spectra of other geometrically frustrated compounds [35].

3.2. Temperature dependent measurements

Unpolarized Raman spectra of CuFeO_2 obtained between 290 and 5 K are presented in figure 4(a). Over this temperature range, no significant change is observed. In particular, no splitting of the E_g mode below T_{N1} is noticeable despite the $R\bar{3}m \rightarrow C2/m$ structural transition at T_{N1} [1, 7, 17]. We attribute this discrepancy to weak resonance with the He–Ne excitation line, which results in the weak intensity of the E_g mode and makes it difficult to resolve any possible splitting. Another possibility is that the temperature of the sample remains above T_{N1} even with a beam power of 4000 W cm^{-2} .

In the case of CuCrO_2 , unpolarized Raman spectra shown in figure 4(b) display noticeable differences as the

temperature is decreased from room temperature down to 8 K. With a close look at the E_g mode at 458 cm^{-1} , one can observe that its tail becomes broader on the right hand side starting below 200 K. With further cooling, an additional mode is easily distinguished and its frequency increases to 470 cm^{-1} at 8 K. This mode is also observed with parallel and cross-polarization configurations (not shown). It should be noted that neutron diffraction [7, 17], magnetostriction [23], and sound velocity measurements (figure 1) do not show any anomaly that could be associated with a structural deformation below 200 K. This mode could have an origin similar to that of the additional modes observed between room temperature and 8 K (figure 4(b)). Moreover, the spectrum of CuCrO_2 at 8 K (figure 4(b)) deserves some attention. Unlike the spectra at other temperatures, it develops a broad background feature centered at $\sim 550\text{ cm}^{-1}$. This broad band, which can also be observed using parallel and cross-polarizations (not shown), might be associated with magnon modes due to a proper screw ordering observed below T_{N2} [36, 37]. Finally, although there is some evidence for a structural deformation at T_{N1} in CuCrO_2 [23], no additional Raman modes are observed below this temperature. Local heating due to the power density of the incident beam (4000 W cm^{-2}) is possible; however, the broad band observed in the spectrum at 8 K (figure 4(b)) clearly shows that the temperature is below T_{N1} . In addition, linewidths of Raman modes normally narrow down with decreasing temperature. For example, in BiFeO_3 , which undergoes a structural transition at the Curie temperature $T_c = 1100\text{ K}$, Fukumura *et al* [38] observed only seven Raman modes at room temperature due to broadening of the modes. All 13 Raman modes were observed only at 4 K, much below T_c [38]. For CuCrO_2 , even lower temperatures and a lower incident beam power might be required for the observation of additional modes. Finally, the ionic displacements might be too small for the observation of additional modes below T_{N1} . This is supported by magnetostriction measurements [23], which show that the strictions along the hexagonal $[110]$ and $[1\bar{1}0]$ axes at 8 K are only $\Delta L/L_{110} \sim 2.5 \times 10^{-4}$ and $\Delta L/L_{1\bar{1}0} \sim 3 \times 10^{-4}$ [23].

Temperature variations of the frequencies of the Raman modes in CuFeO_2 and CuCrO_2 are presented in figure 5. As shown in figure 5(a), the frequencies of both modes in CuFeO_2 increase almost linearly down to 50 K and show a small drop below T_{N1} . In the case of CuCrO_2 (figure 5(b)), the mode frequencies increase between 290 and 80 K. While the A_{1g} mode frequency remains nearly constant between 80 and 8 K, the frequency of the E_g mode slightly softens down to T_{N1} and then remains constant down to 8 K.

As discussed earlier, neutron [17] and x-ray [7] diffraction measurements on CuFeO_2 reveal an $R\bar{3}m \rightarrow C2/m$ structural transition while magnetostriction measurements on CuCrO_2 show evidence for crystal symmetry lowering. In accordance with these results, sound velocity measurements on CuFeO_2 [1] and CuCrO_2 (see figure 1) indicate that both compounds undergo an $R\bar{3}m \rightarrow C2/m$ pseudoproper ferroelastic transition at T_{N1} . According to the group theory [18], one possible scenario is that an E_g -symmetric

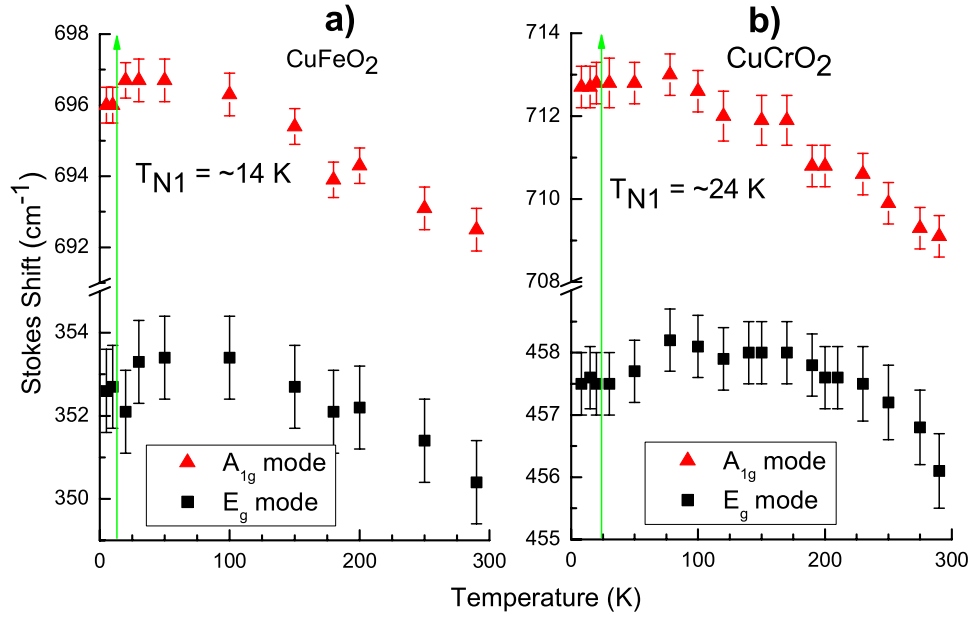


Figure 5. Temperature dependences of the frequencies of the Raman modes in (a) CuFeO₂ and (b) CuCrO₂ could be associated with anharmonic phonon–phonon interactions. Therefore, the E_g modes are not associated with the order parameters of the pseudoproper ferroelastic transitions at T_{N1} in both compounds.

optic mode is associated with the order parameter [1]. In this case, the excess Gibbs free energy G_e can be written as

$$G_e = \frac{1}{2}mw_0^2u^2 + \frac{1}{4}Bu^4 + \frac{1}{2}Ce_s^2 + \gamma e_s u, \quad (3)$$

$$mw_0^2 = a(T - T_0) = A. \quad (4)$$

In the above equations, m is the reduced mass and w_0 is the uncoupled frequency of the soft E_g mode, while a and b are temperature independent constants. The first two terms in equation (3) are due to the Landau expansion of the order parameter u , which corresponds to normal coordinate vibrations associated with the soft E_g optic mode. Thus, the first term $\frac{1}{2}mw_0^2u^2$ corresponds to the harmonic oscillator energy and is the only temperature dependent term. The term $\frac{1}{2}Ce_s^2$ is the elastic energy of the soft acoustic mode associated with the strain component e_s . For simplification, only one elastic constant C is considered (see [1] for complete elastic energy). Finally, the bilinear coupling term $\gamma e_s u$ in equation (3), with γ representing the coupling coefficient, is necessary in order to account for the softening of the acoustic modes observed in CuFeO₂ [1] and CuCrO₂ (see figure 1). After minimizing G_e with respect to u and e_s , one obtains

$$e_s = -\frac{u\gamma}{C} \quad (5)$$

and

$$u = \frac{\sqrt{a(T_0 - T) + \frac{\gamma^2}{C}}}{\sqrt{B}}, \quad (6)$$

which shows that the bilinear coupling term ($\gamma e_s u$) renormalizes the uncoupled transition temperature T_0 to

$$T_{N1} = T_0 + \frac{\gamma^2}{aC}. \quad (7)$$

Finally, the frequency ω of the soft optical mode can be obtained using [39]

$$\omega^2 = \frac{1}{m} \frac{\partial^2 G_e}{\partial u^2}, \quad (8)$$

which yields

$$\omega^2 = \frac{a}{m}(T - T_{N1}) + \frac{\gamma^2}{Cm} \quad (T > T_{N1}) \quad (9)$$

and

$$\omega^2 = \frac{-2a}{m}(T - T_{N1}) + \frac{\gamma^2}{Cm} \quad (T < T_{N1}). \quad (10)$$

According to equations (9) and (10), the frequency square of the soft optical mode should vary linearly with temperature with a slope change at T_{N1} as observed in some pseudoproper ferroelastic compounds [19–22]. According to our Raman measurements, the temperature dependence of the E_g symmetry modes cannot be associated with that of a soft optical mode. Thus, the temperature behavior of all modes is rather attributed to thermal contraction and anharmonic phonon–phonon interactions, in agreement with the analyses of Pavunny *et al* [27] for their Raman study of CuFeO₂ between 400 and 80 K. At lower temperatures, other mechanisms can also play a role in the temperature behavior of the modes. The small drops in the frequencies of Raman modes in CuFeO₂ could be related to ionic displacements due to the structural transition at T_{N1} . However, spin–phonon coupling could also be responsible for the drops in the mode frequencies [40]. In CuCrO₂, the softening of the E_g mode is reminiscent of the findings in RMn₂O₅ (where R = Tb, Eu) [40]. Thus, the temperature dependences of the E_g modes cannot be associated with that of an optic mode driving a pseudoproper ferroelastic transition (equations (9)

and (10)). Our conclusion is that none of the Raman modes in CuFeO₂ and CuCrO₂ can account for the pseudoproper ferroelastic transitions observed at $T_{N1} = 14$ K in CuFeO₂ and at $T_{N1} = 24.3$ K in CuCrO₂. While these results do not refute the pseudoproper ferroelastic transitions in CuFeO₂ [1] and CuCrO₂ (see figure 1), they leave the driving mechanisms unresolved.

4. Conclusions

Polarized Raman scattering measurements were performed on delafossite magnetoelectric CuFeO₂ in order to determine the true nature of the order parameter associated with pseudoproper ferroelastic transition observed in CuFeO₂ by means of sound velocity measurements [1]. As preliminary sound velocity measurements on the isostructural compound CuCrO₂ show similar elastic softening at the antiferromagnetic transition (see figure 1), the Raman measurements were also performed on CuCrO₂ for comparison.

Apart from the vibrational modes in CuFeO₂ and CuCrO₂ with A_{1g} and E_g symmetries, one additional mode in CuFeO₂ and seven additional modes in CuCrO₂ are observed at room temperature. Below 200 K, another mode in CuCrO₂ with a frequency close to that of the E_g mode appears and persists to lower temperatures. The additional modes observed in both compounds are possibly associated with either relaxation of Raman selection rules or crystal field excitations. More interestingly, the spectrum of CuCrO₂ at 8 K shows a broad band centered at 550 cm⁻¹ attributed to the proper screw ordering below T_{N2} . Finally, all modes in both compounds increase in their frequencies with decreasing temperature due to anharmonic phonon–phonon interactions. Therefore, these results show that the E_g symmetry Raman modes in CuFeO₂ and CuCrO₂ do not induce the transitions observed at T_{N1} , leading to the necessity of further search for the true origins of the order parameters associated with the pseudoproper ferroelastic transitions observed at T_{N1} in both compounds.

Acknowledgments

We would like to thank Oleg Petrenko and Serge Jandl for fruitful discussions. This work was supported by grants from the Natural Science and Engineering Research Council of Canada (NSERC) as well as from the Canada Foundation for Innovation (CFI).

References

- [1] Quirion G, Tagore M J, Plumer M L and Petrenko O A 2008 *Phys. Rev. B* **77** 094111
- [2] Kimura T, Lashley J C and Ramirez A P 2006 *Phys. Rev. B* **73** 220401R
- [3] Seki S, Onose Y and Tokura Y 2008 *Phys. Rev. Lett.* **101** 067204
- [4] Quirion G, Plumer M L, Petrenko O A, Balakrishnan G and Proust C 2009 *Phys. Rev. B* **80** 064420
- [5] Kimura K, Nakamura H, Ohgushi K and Kimura T 2008 *Phys. Rev. B* **78** 140401R
- [6] Mitsuda S, Kasahara N, Uno T and Mase M 1998 *J. Phys. Soc. Japan* **67** 4026
- [7] Terada N, Tanaka Y, Tabata Y, Katsumata K, Kikkawa A and Mitsuda S 2006 *J. Phys. Soc. Japan* **75** 113702
- [8] Ajiro Y, Asano T, Takagi T, Meketa M and Goto T 1994 *Physica B* **201** 71
- [9] Terada N *et al* 2007 *Phys. Rev. B* **75** 224411
- [10] Kadowakit H, Takeit H and Motoya K 1995 *J. Phys.: Condens. Matter* **7** 6869
- [11] Poienar M, Damay F, Martin C, Hardy V, Maignan A and André G 2009 *Phys. Rev. B* **79** 014412
- [12] Soda M, Kimura K, Kimura T, Matsuura M and Hirota H 2009 *J. Phys. Soc. Japan* **78** 124703
- [13] Katsura H, Nagaosa N and Balatsky A V 2005 *Phys. Rev. Lett.* **95** 057205
- [14] Mostovoy M 2006 *Phys. Rev. Lett.* **96** 067601
- [15] Arima T 2007 *J. Phys. Soc. Japan* **76** 073702
- [16] Quirion G, Tagore M J, Plumer M L and Petrenko O A 2009 *J. Phys.: Conf. Ser.* **145** 012070
- [17] Ye F, Ren Y, Huang Q, Fernandez-Baca J A, Dai P, Lynn J W and Kimura T 2006 *Phys. Rev. B* **73** 220404R
- [18] Tinkhan M 2003 *Group Theory and Quantum Mechanics* (New York: Dover)
- [19] Aktas O, Clouter M J and Quirion G 2009 *J. Phys.: Condens. Matter* **21** 285901
- [20] Quirion G, Wu W, Aktas O, Rideout J, Clouter M J and Mróz B 2009 *J. Phys.: Condens. Matter* **21** 455901
- [21] Hellwig H, Goncharov A F, Gregoryanz E, Mao H K and Hemley R J 2003 *Phys. Rev. B* **67** 174110
- [22] Errandonea G and Savary H 1981 *Phys. Rev. B* **24** 1292
- [23] Kimura K, Otani T, Nakamura H, Wakabashi Y and Kimura T 2009 *J. Phys. Soc. Japan* **78** 113710
- [24] Petrenko O A, Balakrishnan G, Lees M R, Paul D M and Hoser A 2000 *Phys. Rev. B* **62** 8983
- [25] Pellicer-Porres J, Segura A, Martínez E, Saitta A M, Polian A, Chervin J C and Canny B 2005 *Phys. Rev. B* **72** 064301
- [26] Pavunny S P, Kumar A, Thomas R, Murari N M and Katiyar R S 2009 *Mater. Res. Soc. Symp. Proc.* **1183** 14
- [27] Pavunny S J, Kumar A and Katiyar R S 2010 *J. Appl. Phys.* **107** 013522
- [28] Julien C and Massot M 2002 *Solid State Ion.* **148** 53
- [29] Decius J C and Hexter R M 1997 *Molecular Vibrations in Crystals* (New York: McGraw-Hill)
- [30] Shua J, Zhua X and Yid T 2009 *Electrochim. Acta* **54** 2795
- [31] Amami M, Jlaiel F, Strobel P and Salah A B 2011 *Mater. Res. Bull.* **46** 1729
- [32] Zheng S H, Jiang G S, Su J R and Zhu C F 2006 *Mater. Lett.* **60** 3871
- [33] Huang H, Zhu C F and Liu W 2004 *Chin. J. Chem. Phys.* **17** 161
- [34] Pellicer-Porres J, Martínez-García J, Segura A, Rodríguez-Hernández P, Muñoz A, Chervin J C, Garro N and Kim D 2006 *Phys. Rev. B* **74** 184301
- [35] Lummen T T A, Handayani I P, Donker M C, Fausti D, Dhalenne G, Berthet P, Revcolevschi A and van Loosdrecht P H M 2008 *Phys. Rev. B* **77** 214310
- [36] Poienar M, Damay F, Martin C, Robert J and Petit S 2010 *Phys. Rev. B* **81** 104411
- [37] Kajimoto R, Nakajima K, Ohira-Kawamura S, Inamura Y, Kakurai K, Arai M, Hokazono T, Satoshi S and Okuda T 2010 *J. Phys. Soc. Japan* **79** 123705
- [38] Fukumura H, Matsui S, Harima H, Takahashi T, Itoh T, Kisoda K, Tamada M, Noguchi Y and Miyayama M 2007 *J. Phys.: Condens. Matter* **19** 365224
- [39] David W I F 1983 *J. Phys. C: Solid State Phys.* **16** 5093
- [40] García-Flores A F, Granado E, Martinho H, Urbano R R, Rettori C, Golovenchits E I, Sanina V A, Oseroff S B, Park S and Cheong S W 2006 *Phys. Rev. B* **73** 104411